,,, , ,,

Indirect excitons and trions in $MoSe_2/WSe_2$ van der Waals heterostructures

E. V. Calman*,[1] L. H. Fowler-Gerace*,[1] D. J. Choksy,[1] L. V. Butov,[1]
D. E. Nikonov,[2] I. A. Young,[2] S. Hu,[3] A. Mishchenko,[3] and A. K. Geim[3]

[1]*Department of Physics, University of California at San Diego, La Jolla, CA 92093, USA*
[2]*Components Research, Intel Corporation, Hillsboro, OR 97124 USA*
[3]*School of Physics and Astronomy, University of Manchester, Oxford Road, Manchester M13 9PL, UK*

Indirect excitons (IX) in semiconductor heterostructures are bosons, which can cool below the temperature of quantum degeneracy and can be effectively controlled by voltage and light. IX quantum Bose gases and IX devices were explored in GaAs heterostructures where an IX range of existence is limited to low temperatures due to low IX binding energies. IXs in van der Waals transition-metal dichalcogenide (TMD) heterostructures are characterized by large binding energies giving the opportunity for exploring excitonic quantum gases and for creating excitonic devices at high temperatures. TMD heterostructures also offer a new platform for studying single-exciton phenomena and few-particle complexes. In this work, we present studies of IXs in $MoSe_2/WSe_2$ heterostructures and report on two IX luminescence lines whose energy splitting and temperature dependence identify them as neutral and charged IXs. The experimentally found binding energy of the indirect charged excitons, i.e. indirect trions, is close to the calculated binding energy of 28 meV for negative indirect trions in TMD heterostructures [Deilmann, Thygesen, Nano Lett. 18, 1460 (2018)]. We also report on the realization of IXs with a luminescence linewidth reaching 4 meV at low temperatures. An enhancement of IX luminescence intensity and the narrow linewidth are observed in localized spots.

PACS numbers:

An indirect exciton (IX), also known as an interlayer exciton, is a bound pair of an electron and a hole confined in spatially separated layers. The spatial separation between the electron and hole layers allows achieving long IX lifetimes, orders of magnitude longer than lifetimes of direct excitons (DXs) [1]. Due to their long lifetimes, IXs can cool below the temperature of quantum degeneracy [2]. The realization of IX quantum Bose gases in GaAs heterostructures led to finding of many phenomena, including spontaneous coherence and condensation of IXs [3], the spatially modulated exciton state [4, 5], the commensurability effect of exciton density waves [6], spin textures [7], and the Pancharatnam-Berry phase and long-range coherent spin transport in the IX condensate [8].

Furthermore, an IX has a built-in electric dipole moment, ed (d is the separation between the electron and hole layers). As a result, IX energy, lifetime, and flux can be effectively controlled by voltage that is explored for the development of excitonic devices. In GaAs heterostructures, experimental proof-of-principle demonstrations were performed for excitonic ramps [9, 10], excitonic acoustic-wave [11] and electrostatic [12] conveyers, and excitonic transistors [13].

However, the IX range of existence in GaAs heterostructures is limited to low temperatures due to low IX binding energies. Excitons exist in the temperature range roughly below E_{ex}/k_B (E_{ex} is the exciton binding energy, k_B is the Boltzmann constant) [14]. The IX binding energy in GaAs/AlGaAs heterostructures is typically ~ 4 meV [15]. The maximum E_{ex} in GaAs heterostructures is achieved in GaAs/AlAs coupled quantum wells (CQW) and is ~ 10 meV [16]. The temperature of quantum degeneracy, which can be achieved with increasing density before excitons dissociation to electron-hole plasma, also scales proportionally to E_{ex} [17]. In GaAs heterostructures, quantum degeneracy was achieved below few Kelvin [2] and the proof of principle for the operation of IX switching devices was demonstrated below ~ 100 K [18]. IXs with high E_{ex} reaching ~ 30 meV are explored in ZnO and GaN heterostructures [19–22].

Van der Waals heterostructures composed of atomically thin layers of TMD offer an opportunity to realize artificial materials with designable properties [23] and, in particular, allow the realization of excitons with remarkably high binding energies [24, 25]. IXs in TMD heterostructures are characterized by binding energies exceeding 100 meV making them stable at room temperature [17]. IXs were observed at room temperature in TMD heterostructures [26]. Due to the high IX binding energy, TMD heterostructures can form a material platform both for exploring high-temperature quantum Bose gases of IXs and for creating realistic excitonic devices.

IXs are instensively studied in optically excited van der Waals TMD heterostructures with coupled electron and hole layers [26–53]. IXs can also appear in electron-electron (or hole-hole) bilayers in a collective electronic state in strong magnetic fields at the total Landau level

[84] *These authors contributed equally to this work

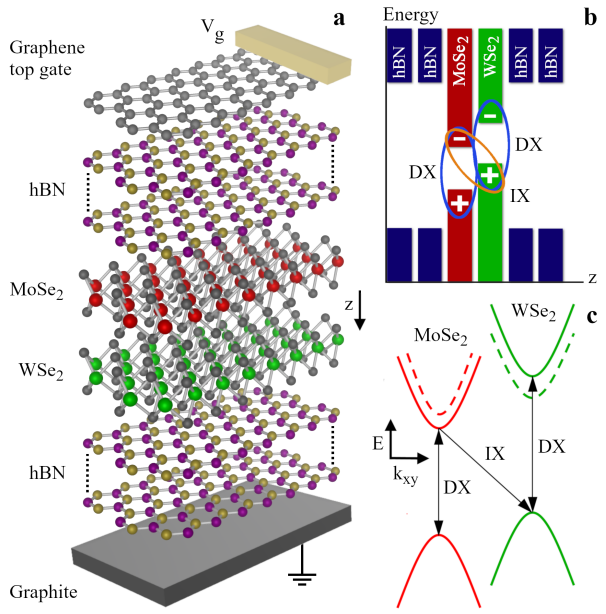

FIG. 1: **Van der Waals $MoSe_2$/WSe_2 heterostructure.** The heterostructure layer (a) and real space energy band (b) diagrams. The ovals indicate a direct exciton (DX) and an indirect exciton (IX) composed of an electron (−) and a hole (+). (c) Momentum space energy band diagram around the K point. Solid and dashed lines represent spin-up and spin-down bands. Optically active low-energy DX and IX states are indicated by arrows.

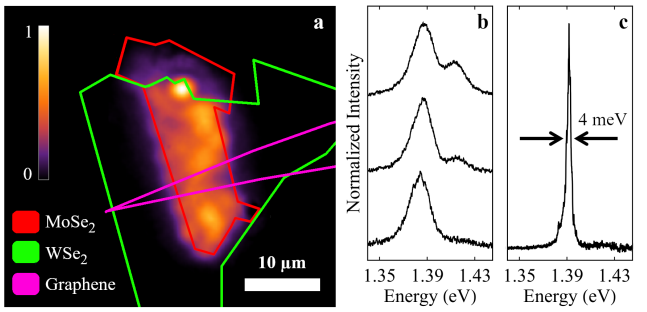

FIG. 2: **Spatially indirect, i.e., interlayer, luminescence in CQW flake and bright spot.** (a) x-y map of indirect luminescence (spectral range 1.24–1.46 eV) in sample S. Indirect luminescence intensity is enhanced in a bright spot observed near the top of the CQW flake. The layer boundaries are shown. (b) The luminescence spectrum at the CQW flake in sample S at excitation power P_{ex} = 3.4, 1, and 0.5 mW (top to bottom). (c) The luminescence spectrum at the bright spot in sample M at P_{ex} = 10 μW. The laser excitation is defocused in (a) and focused at the flake center in sample S (b) and at the bright spot in sample M (c). T = 1.7 K, V_g = 0. All luminescence intensities are normalized.

filling factor 1. The latter was realized in GaAs heterostructures [54–59] and in graphene–boron-nitride–graphene van der Waals heterostructures [60, 61].

In this work, we present studies of IXs in $MoSe_2$/WSe_2 heterostructures. We report on the observation of charged IXs, i.e. indirect trions (IX^T). The identification of indirect trions is based on the measured energy splitting and temperature dependence of IX and IX^T luminescence lines: The splitting corresponds to the binding energy for negative indirect trions in TMD heterostructures calculated in Ref. [62] and the temperature dependence follows the mass action law for the indirect trions. We also report on the realization of IXs with a luminescence linewidth reaching 4 meV at low temperatures, the lowest value reported so far for IXs in TMD heterostructures. An enhancement of IX luminescence intensity and the narrow linewidth are observed in localized spots.

The $MoSe_2$/WSe_2 heterostructures were assembled by stacking mechanically exfoliated 2D crystals on a graphite substrate (Fig. 1a). The CQW is formed where the $MoSe_2$ and WSe_2 monolayers overlap. The $MoSe_2$ and WSe_2 monolayers are encapsulated by hexagonal boron nitride (hBN) serving as dielectric cladding layers. The real-space energy-band diagram is shown in Fig. 1b. IXs are formed from electrons and holes confined in adjacent monolayer $MoSe_2$ and WSe_2, respectively. These type-II $MoSe_2$/WSe_2 heterostructures with staggered band alignment are similar to AlAs/GaAs CQW where IXs are formed from electrons and holes confined in adjacent AlAs and GaAs layers, respectively [16, 18]. In the $MoSe_2$/WSe_2 heterostructures, due to the order of spin-up and spin-down states in valence and conduction bands (VB and CB) the lowest energy DX state is optically active in $MoSe_2$ and dark in WSe_2, and the lowest energy IX state is optically active (Fig. 1c) [52, 53, 63–67]. We studied heterostructures manufactured in Manchester and San Diego (samples M and S). The order of $MoSe_2$ and WSe_2 layers is different in samples M and S to probe both configurations. Both samples show indirect trions and intensity enhancement in localized spots.

Along most of the CQW heterostructure area, the IX luminescence intensity varies only slightly (Fig. 2a). We will refer to this CQW heterostructure area as the CQW flake. However, we observed bright spots, which exhibit enhanced IX luminescence in comparison to the surrounding regions of the CQW heterostructure [Fig. 2a and Figs. S1 and S2 in Supplementray Information (SI)]. The CQW flakes and CQW bright spots show similar features of neutral and charged IX luminenscence and the data for both these regions are presented in this work.

In this paragraph, we outline phenomenological properties of the bright spots. We note that further details of their properties and their origin form the subject for future studies and do not affect the conclusions on neutral and charged IXs in this work. The enhancement of IX luminescence at the bright spots is localized within ~ 2 μm in sample S and within the length smaller than the 1 μm optics resolution in sample M. In contrast to

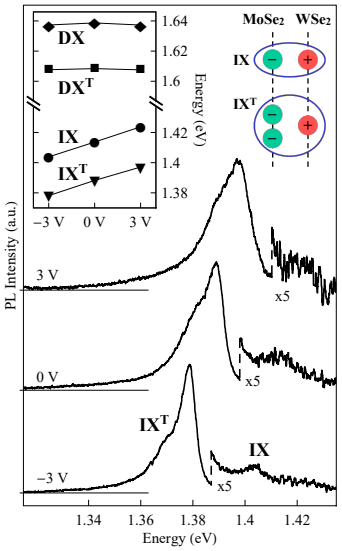

FIG. 3: **Gate voltage dependence.** Indirect luminescence spectra in $MoSe_2/WSe_2$ CQW at different gate voltages V_g at the bright spot in sample M. Left inset: Luminescence peak energy vs. V_g. IX and IX^T are indirect exciton and trion, DX and DX^T are direct exciton and trion. Right inset: Schematic of IX and IX^T. P_{ex} = 1.25 mW, T = 1.7 K.

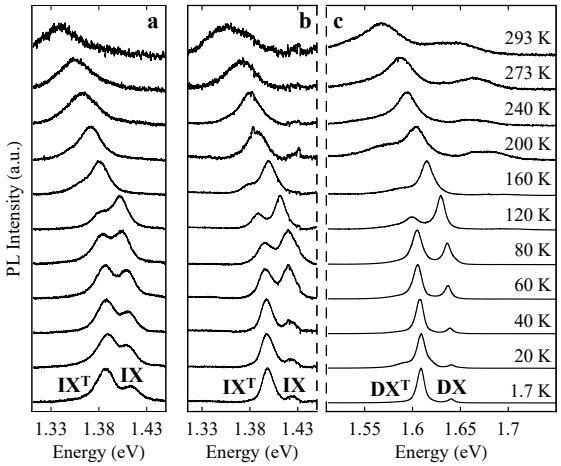

FIG. 4: **Temperature dependence.** Spectra of spatially indirect (a,b) and direct (c) luminescence in $MoSe_2/WSe_2$ CQW at different temperatures at CQW flake in sample S (a) and bright spot in sample M (b,c). P_{ex} = 3.4 (a) and 1.25 (b,c) mW, V_g = 0.

IX luminescence, the intralayer DX luminescence varies only slightly along the CQW heterostructure and does not show an intensity enhancement in the bright spots [Figs. S1 and S2 in SI]. The bright spots form naturally with no artificially designed IX confinement such as in electrostatic traps in GaAs heterostructures [68–74]. The presence of the luminescence bright spot for IXs with a built-in electric dipole and its absence for DXs with no electric dipole suggests that the bright spots originate from an accidental IX trapping due to the background electrostatic potential in the heterostructures. The bright spot shows a narrow IX linewidth reaching 4 meV at the lowest excitation power tested (Figs. 2c and S3). The IX linewidth in the bright spot is smaller than the IX linewidths in the rest of the sample. The lowest IX linewidth in the CQW flakes outside the bright spot is observed at the lowest excitation power tested and is 15 (21) meV for the higher- (lower)-energy IX line (Figs. 2b, S12).

Two lines of spatially indirect luminescence are observed in the spectrum (Figs. 2b, 3). Due to the IX electric dipole moment, ed, the IX energy shifts in the voltage-induced electric field in the z direction, F_z, by $\delta E = -edF_z$. The energy of two luminescence lines is controlled by voltage V_g applied between the graphene top gate and graphite back gate and creating the bias across the CQW structure (Fig. 3), indicating that both these lines correspond to spatially indirect luminescence.

The IX line splitting of 28 meV (sample S, Fig. 2b) [26 meV (sample M, Fig. 3)] is much smaller than the WSe_2 VB spin-orbit splitting [75]. Therefore, both IX transitions involve holes in the upper VB subband (B excitons considered in Ref. [75] are not involved).

The measured energy splitting and temperature dependence of these two lines identify them as neutral and charged indirect excitons. The lower energy line corresponds to charged IXs, i.e., indirect trions (IX^T), and the higher energy line to neutral IXs (Fig. 3 right inset).

The energy of the trion luminescence is determined by the difference between the initial state, trion, and final state, remaining electron (for negative trions). At low densities, the IX and IX^T luminescence energies should experience the same shift with voltage following the gap between the VB of WSe_2 and the CB of $MoSe_2$ [62], consistent with the experiment (Fig. 3). The splitting between the lines corresponds to the trion binding energy. Details are presented in SI. The experimentally found binding energy of the indirect trions of 26–28 meV is in agreement with the calculated binding energy of 28 meV for negative indirect trions in MoS_2/WS_2 heterostructures [62].

Similarly, spatially direct neutral and charged excitons, DX and DX^T, are observed for spatially direct, i.e., intralayer, luminescence (Fig. 4c). However, in contrast to IX and IX^T, the peak energy of DX and DX^T practically does not change with voltage due to vanishing built-in dipole moment in the direction of applied electric field for direct excitons and trions (Fig. 3 left inset).

The measured indirect trion binding energy of 26–28 meV is smaller than the direct trion binding energy of 32 meV (Fig. 4) due to the separation between the electron and hole layers, consistent with the theory of indirect trions in GaAs and TMD heterostructures [62, 76, 77]. DX and DX^T luminescence was studied earlier in mono-

layer $MoSe_2$ [66, 67, 78–81].

Further significant support for the asignment of the two lines of spatially indirect luminescence to neutral and charged indirect excitons comes from the temperature dependence: The luminescence intensity ratio of the lines IX^T/IX decreases with increasing temperature (Fig. 4a,b, Fig. 5a red symbols, and Fig. 5b symbols) in agreement with the mass action law for the indirect trions (Fig. 5a red line and Fig. 5b lines). The relative intensity of the IX^T luminescence decreases with temperature due to the thermal dissociation of trions. The IX^T temperature dependence is similar to that for DX^T both in earlier studies of DX^T in $MoSe_2$ monolayers [79] and in this work (Figs. 4 and 5).

Solid lines in Fig. 5 present the simulated ratios of trion and exciton integrated luminescence intensities for the direct, DX^T/DX, and the indirect, IX^T/IX, cases. We simulated these ratios using their approximate proportionality to the densities of corresponding particles. The dependence of the densities on temperature is obtained from the mass action model [79], details are presented in SI. In these simulations, the trion binding energy is taken from the measured line splitting. The simulations include two fitting parameters: the densities of background charge carriers n_B and photoexcited electron-hole pairs n_P, their estimation is described in SI. The simulations give qualitatively similar results for various n_P and n_B: At high temperatures, the ratio of trion and exciton densities n_T/n_X increases with reducing temperature, however, at low temperatures, n_T/n_X saturates (Figs. 5 and S8). This saturation is the key characteristic of trion luminescence. The origin of this saturation is in the finite number of background electrons that are invlolved in the trions. For the trions formed by binding of the background electrons with photoexcited excitons, at low temperatures, the trion density saturates at n_B and, in turn, the ratio n_T/n_X asymptotically approaches $n_B/(n_P - n_B)$. The simulations are in agreement with the experimental data both for direct and indirect trions in the entire temperature range (Fig. 5).

As in the type-I MoS_2/hBN TMD heterostructure [26], IXs are observed at room temperature in our type-II heterostructures (Fig. 4). The observed red shift of the lines with increasing temperature (Fig. 4) originates from the band gap reduction, which is typical for semiconductors, the TMDs included [79].

The narrowest indirect luminescence linewidth is observed at the lowest temperature (Fig. 4) and smallest excitation power P_{ex} (Fig. S3). The indirect luminescence broadens up to $\sim$ 40 meV at room temperature (Fig. 4). With increasing P_{ex}, the indirect luminescence broadens and shifts to higher energies (Figs. 2, S3). Similar line broadening and shift to higher energies were observed for IXs in GaAs heterostructures and described in terms of repulsive IX interaction [70], which originates from the repulsion of oriented electric dipoles [82–84]. Increasing

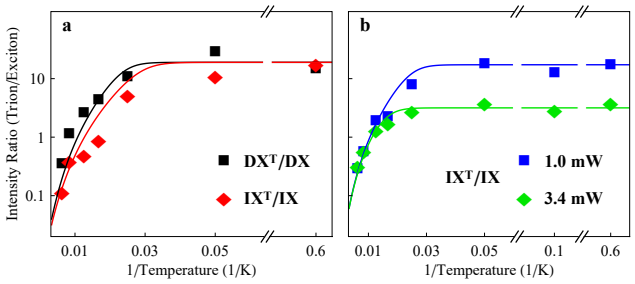

FIG. 5: **Temperature dependence.** Experimental (symbols) and simulated (lines) spectrally integrated luminescence intensity ratio IX^T/IX (green, blue, red) and DX^T/DX (black) vs. 1/temperature at the CQW bright spot in sample M (a) and the CQW flake in sample S (b). P_{ex} = 1.25 mW (a), 1 mW [blue squares in (b)], and 3.4 mW [green diamonds in (b)], V_g = 0.

the density with P_{ex} leads to the enhancement of interaction in the system of indirect excitons and trions and, in turn, the enhancement of IX^T and IX energies.

Isolated IX^T have substantial binding energy at low separation between electron and hole layers [62, 76, 77], relevant for the $MoSe_2/WSe_2$ heterostructure. However, the IX^T binding energy is smaller than the IX binding energy that stabilizes the neutral system of IXs against IX transformations to trions and charged particles. This suggests that most of IX^T form by binding of electrons and holes created by excitation to background charge carriers which are present in the heterostructure due to unintentional doping and CQW layer charging induced by voltage. Increasing P_{ex} leads to the enhancement of relative intensity of IX line, i.e. reduction of IX^T/IX ratio, at low temperatures (Figs. 2b, 5b), consistent with the trion density saturation at n_B and, as a result, enhanced fraction of IXs with increased n_P.

We also briefly discuss alternative intepretations for the two lines of spatially indirect luminescence. A splitting of IX or DX emission to two luminescence lines is a general phenomenon in two coupled TMD layers. Various interpretations based on the assignment of the lines to different states of neutral excitons were offered to explain this splitting: The interpretations in terms of (i) excitonic states split due to the CB K-valley spin splitting [29], (ii) excitonic states indirect in momentum space and split due to the valley energy difference [32, 38] or spin-orbit coupling [39], and (iii) excitonic states in moiré superlattice [43–48] following the theory of moiré IXs and DXs [50–52].

However, interpretations based on different states of neutral excitons, including interpretations (i)-(iii) outlined above, do not offer a good agreement with the experimental data in Fig. 5 and, in turn, a plausible explanation for the IX lines in the studied heterostructures. As detailed in SI, for different states of neutral excitons, the relative occupation of the lower-energy state and, as a re-

sult, the relative intensity of the lower-energy line should increase by orders of magnitude with lowering the temperature in the range $1/T = 0.03 - 0.6$ 1/K (Fig. S10). However, the experimental data (Figs. 5, S6, and S10) show the nearly constant relative intensity of the lower-energy line in this temperature range. In contrast, the theory of neutral excitons and trions is in agreement with the data (Figs. 5, S6, and S10). The large discrepancy, by orders of magnitude, between the interpretations of the two indirect luminescence lines based on two different states of neutral IXs and the experimental data, indicates that these interpretations are less plausible than the interpretation based on neutral exciton IX and trion IX^T that is in agreement with the data (Figs. 5, S6, and S10).

In conclusion, we present studies of $MoSe_2/WSe_2$ heterostructures and report on two lines of spatially indirect luminescence whose energy splitting and temperature dependence identify them as neutral indirect excitons and charged indirect excitons, i.e. indirect trions.

Acknowledgements. We thank Michael Fogler for discussions. These studies were supported by DOE Office of Basic Energy Sciences under award DE-FG02-07ER46449 and the device fabrication and data analysis were supported by NSF Grants 1905478 and 1640173 and NERC, a subsidiary of SRC, through the SRC-NRI Center for Excitonic Devices.

References

[1] Yu.E. Lozovik, V.I. Yudson, A new mechanism for superconductivity: pairing between spatially separated electrons and holes, *Sov. Phys. JETP* **44**, 389 (1976).

[2] L.V. Butov, A.L. Ivanov, A. Imamoglu, P.B. Littlewood, A.A. Shashkin, V.T. Dolgopolov, K.L. Campman, A.C. Gossard, Stimulated scattering of indirect excitons in coupled quantum wells: Signature of a degenerate Bose-gas of excitons, *Phys. Rev. Lett.* **86**, 5608 (2001).

[3] A.A. High, J.R. Leonard, A.T. Hammack, M.M. Fogler, L.V. Butov, A.V. Kavokin, K.L. Campman, A.C. Gossard, Spontaneous coherence in a cold exciton gas, *Nature* **483**, 584 (2012).

[4] L.V. Butov, A.C. Gossard, D.S. Chemla, Macroscopically ordered state in an exciton system, *Nature* **418**, 751 (2002).

[5] M. Alloing, M. Beian, M. Lewenstein, D. Fuster, Y. González, L. González, R. Combescot, M. Combescot, F. Dubin, Evidence for a Bose-Einstein condensate of excitons, *Europhys. Lett.* **107**, 10012 (2014).

[6] Sen Yang, L.V. Butov, B.D. Simons, K.L. Campman, A.C. Gossard, Fluctuation and Commensurability Effect of Exciton Density Wave, *Phys. Rev. B* **91**, 245302 (2015).

[7] A.A. High, A.T. Hammack, J.R. Leonard, Sen Yang, L.V. Butov, T. Ostatnický, M. Vladimirova, A.V. Kavokin, T.C.H. Liew, K.L. Campman, A.C. Gossard, Spin currents in a coherent exciton gas, *Phys. Rev. Lett.* **110**, 246403 (2013).

[8] J.R. Leonard, A.A. High, A.T. Hammack, M.M. Fogler, L.V. Butov, K.L. Campman, A.C. Gossard, Pancharatnam-Berry phase in condensate of indirect excitons, *Nature Commun.* **9**, 2158 (2018).

[9] M. Hagn, A. Zrenner, G. Böhm, G. Weimann, Electric-field-induced exciton transport in coupled quantum well structures, *Appl. Phys. Lett.* **67**, 232 (1995).

[10] A. Gärtner, A.W. Holleitner, J.P. Kotthaus, D. Schuh, Drift mobility of long-living excitons in coupled GaAs quantum wells, *Appl. Phys. Lett.* **89**, 052108 (2006).

[11] S. Lazić, A. Violante, K. Cohen, R. Hey, R. Rapaport, P.V. Santos, Scalable interconnections for remote indirect exciton systems based on acoustic transport, *Phys. Rev. B* **89**, 085313 (2014).

[12] A.G. Winbow, J.R. Leonard, M. Remeika, Y.Y. Kuznetsova, A.A. High, A.T. Hammack, L.V. Butov, J. Wilkes, A.A. Guenther, A.L. Ivanov, M. Hanson, A.C. Gossard, Electrostatic Conveyer for Excitons, *Phys. Rev. Lett.* **106**, 196806 (2011).

[13] A.A. High, E.E. Novitskaya, L.V. Butov, M. Hanson, A.C. Gossard, Control of exciton fluxes in an excitonic integrated circuit, *Science* **321**, 229 (2008).

[14] D.S. Chemla, D.A.B. Miller, P.W. Smith, A.C. Gossard, W. Wiegmann, Room temperature excitonic nonlinear absorption and refraction in GaAs/AlGaAs multiple quantum well structures, *IEEE J. Quantum Electron.* **20**, 265-275 (1984).

[15] K. Sivalertporn, L. Mouchliadis, A.L. Ivanov, R. Philp, E.A. Muljarov, Direct and indirect excitons in semiconductor coupled quantum wells in an applied electric field, *Phys. Rev. B* **85**, 045207 (2012).

[16] A. Zrenner, P. Leeb, J. Schäfler, G. Böhm, G. Weimann, J.M. Worlock, L.T. Florez, J.P. Harbison, Indirect excitons in coupled quantum well structures, *Surf. Sci.* **263**, 496-501 (1992).

[17] M.M. Fogler, L.V. Butov, K.S. Novoselov, High-temperature superfluidity with indirect excitons in van der Waals heterostructures, *Nature Commun.* **5**, 4555 (2014).

[18] G. Grosso, J. Graves, A.T. Hammack, A.A. High, L.V. Butov, M. Hanson, A.C. Gossard, Excitonic switches operating at around 100 K, *Nature Photonics* **3**, 577-580 (2009).

[19] P. Lefebvre, S. Kalliakos, T. Bretagnon, P. Valvin, T. Taliercio, B. Gil, N. Grandjean, J. Massies, Observation and modeling of the time-dependent descreening of internal electric field in a wurtzite $GaN/Al_{0.15}Ga_{0.85}N$ quantum well after high photoexcitation, *Phys. Rev. B* **69**, 035307 (2004).

[20] C. Morhain, T. Bretagnon, P. Lefebvre, X. Tang, P. Valvin, T. Guillet, B. Gil, T. Taliercio, M. Teisseire-Doninelli, B. Vinter, C. Deparis, Internal electric field in wurtzite $ZnO/Zn_{0.78}Mg_{0.22}O$ quantum wells, *Phys. Rev. B* **72**, 241305(R) (2005).

[21] F. Fedichkin, T. Guillet, P. Valvin, B. Jouault, C. Brimont, T. Bretagnon, L. Lahourcade, N. Grandjean, P. Lefebvre, M. Vladimirova, Room-Temperature Transport of Indirect Excitons in (Al,Ga)N/GaN Quantum Wells, *Phys. Rev. Appl.* **6**, 014011 (2016).

[22] François Chiaruttini, Thierry Guillet, Christelle Brimont, Benoit Jouault, Pierre Lefebvre, Jessica Vives, Sebastien Chenot, Yvon Cordier, Benjamin Damilano, Maria Vladimirova, Trapping Dipolar Exciton Fluids in GaN/(AlGa)N Nanostructures, *Nano Lett.* 10.1021/acs.nanolett.9b00914 (2019).

[23] A.K. Geim, I.V. Grigorieva, Van der Waals heterostructures, *Nature* **499**, 419-425 (2013).

[24] Ziliang Ye, Ting Cao, Kevin O'Brien, Hanyu Zhu, Xiaobo Yin, Yuan Wang, Steven G. Louie, Xiang Zhang, Probing excitonic dark states in single-layer tungsten disulphide, *Nature* **513**, 214-218 (2014).

[25] Alexey Chernikov, Timothy C. Berkelbach, Heather M. Hill, Albert Rigosi, Yilei Li, Ozgur Burak Aslan, David R. Reichman, Mark S. Hybertsen, Tony F. Heinz, Exciton Binding Energy and Nonhydrogenic Rydberg Series in Monolayer WS_2, *Phys. Rev. Lett.* **113**, 076802 (2014).

[26] E.V. Calman, M.M. Fogler, L.V. Butov, S. Hu, A. Mishchenko, A.K. Geim, Indirect excitons in van der Waals heterostructures at room temperature, *Nature Commun.* **9**, 1895 (2018).

[27] Hui Fang, Corsin Battaglia, Carlo Carraro, Slavomir Nemsak, Burak Ozdol, Jeong Seuk Kang, Hans A. Bechtel, Sujay B. Desai, Florian Kronast, Ahmet A. Unal, Giuseppina Conti, Catherine Conlon, Gunnar K. Palsson, Michael C. Marting, Andrew M. Minor, Charles S. Fadley, Eli Yablonovitch, Roya Maboudian, Ali Javey, Strong interlayer coupling in van der Waals heterostructures built from single-layer chalcogenides, *PNAS* **111**, 6198 (2014).

[28] Xiaoping Hong, Jonghwan Kim, Su-Fei Shi, Yu Zhang, Chenhao Jin, Yinghui Sun, Sefaattin Tongay, Junqiao Wu, Yanfeng Zhang, Feng Wang, Ultrafast charge transfer in atomically thin MoS_2/WS_2 heterostructures, *Nature Nano.* **9**, 682-686 (2014).

[29] Pasqual Rivera, John R. Schaibley, Aaron M. Jones, Jason S. Ross, Sanfeng Wu, Grant Aivazian, Philip Klement, Kyle Seyler, Genevieve Clark, Nirmal J. Ghimire, Jiaqiang Yan, D.G. Mandrus, Wang Yao, Xiaodong Xu, Observation of long-lived interlayer excitons in monolayer $MoSe_2$-WSe_2 heterostructures, *Nature Commun.* **6**, 6242 (2015).

[30] Hongyi Yu, Yong Wang, Qingjun Tong, Xiaodong Xu, Wang Yao, Anomalous Light Cones and Valley Optical Selection Rules of Interlayer Excitons in Twisted Heterobilayers, *Phys. Rev. Lett.* **115**, 187002 (2015).

[31] Pasqual Rivera, Kyle L. Seyler, Hongyi Yu, John R. Schaibley, Jiaqiang Yan, David G. Mandrus, Wang Yao, Xiaodong Xu, Valley-polarized exciton dynamics in a 2D semiconductor heterostructure, *Science* **351**, 688-691 (2016).

[32] Bastian Miller, Alexander Steinhoff, Borja Pano, Julian Klein, Frank Jahnke, Alexander Holleitner, Ursula Wurstbauer, Long-Lived Direct and Indirect Interlayer Excitons in van der Waals Heterostructures, *Nano Lett.* **17**, 5229-5237 (2017).

[33] Philipp Nagler, Gerd Plechinger, Mariana V. Ballottin, Anatolie Mitioglu, Sebastian Meier, Nicola Paradiso, Christoph Strunk, Alexey Chernikov, Peter C.M. Christianen, Christian Schüller, Tobias Korn, Interlayer exciton dynamics in a dichalcogenide monolayer heterostructure, *2D Mater.* **4**, 025112 (2017).

[34] Shiyuan Gao, Li Yang, Catalin D. Spataru, Interlayer Coupling and Gate-Tunable Excitons in Transition Metal Dichalcogenide Heterostructures, *Nano Lett.* **17**, 7809-7813 (2017).

[35] Engin Torun, Henrique P.C. Miranda, Alejandro Molina-Sánchez, Ludger Wirtz, Interlayer and intralayer excitons in MoS_2/WS_2 and $MoSe_2/WSe_2$ heterobilayers, *Phys. Rev. B* **97**, 245427 (2018).

[36] Dmitrii Unuchek, Alberto Ciarrocchi, Ahmet Avsar, Kenji Watanabe, Takashi Taniguchi, Andras Kis, Room-temperature electrical control of exciton flux in a van der Waals heterostructure, *Nature* **560**, 340 (2018).

[37] Zefang Wang, Yi-Hsin Chiu, Kevin Honz, Kin Fai Mak, Jie Shan, Electrical Tuning of Interlayer Exciton Gases in WSe_2 Bilayers, *Nano Lett.* **18**, 137-143 (2018).

[38] Mitsuhiro Okada, Alex Kutana, Yusuke Kureishi, Yu Kobayashi, Yuika Saito, Tetsuki Saito, Kenji Watanabe, Takashi Taniguchi, Sunny Gupta, Yasumitsu Miyata, Boris I. Yakobson, Hisanori Shinohara, Ryo Kitaura, Direct and Indirect Interlayer Excitons in a van der Waals Heterostructure of hBN/WS_2/MoS_2/hBN, *ACS Nano* **12**, 2498-2505 (2018).

[39] Aubrey T. Hanbicki, Hsun-Jen Chuang, Matthew R. Rosenberger, C. Stephen Hellberg, Saujan V. Sivaram, Kathleen M. McCreary, Igor I. Mazin, Berend T. Jonker, Double Indirect Interlayer Exciton in a $MoSe_2/WSe_2$ van der Waals Heterostructure, *ACS Nano* **12**, 4719-4726 (2018).

[40] Chongyun Jiang, Weigao Xu, Abdullah Rasmita, Zumeng Huang, Ke Li, Qihua Xiong, Wei-bo Gao, Microsecond dark-exciton valley polarization memory in two-dimensional heterostructures, *Nature Commun.* **9**, 753 (2018).

[41] Chanyeol Choi, Jiahui Huang, Hung-Chieh Cheng, Hyunseok Kim, Abhinav Kumar Vinod, Sang-Hoon Bae, V. Ongun Özçelik, Roberto Grassi, Jongjae Chae, Shu-Wei Huang, Xiangfeng Duan, Kristen Kaasbjerg, Tony Low, Chee Wei Wong, Enhanced interlayer neutral excitons and trions in trilayer van der Waals heterostructures, *2D Materials and Applications* **2** 30 (2018).

[42] Luis A. Jauregui, Andrew Y. Joe, Kateryna Pistunova, Dominik S. Wild, Alexander A. High, You Zhou, Giovanni Scuri, Kristiaan De Greve, Andrey Sushko, Che-Hang Yu, Takashi Taniguchi, Kenji Watanabe, Daniel J. Needleman, Mikhail D. Lukin, Hongkun Park, Philip Kim, Electrical control of interlayer exciton dynamics in atomically thin heterostructures, arXiv:1812.08691

[43] Nan Zhang, Alessandro Surrente, Michal Baranowski, Duncan K. Maude, Patricia Gant, Andres Castellanos-Gomez, Paulina Plochocka, Moiré Intralayer Excitons in a $MoSe_2/MoS_2$ Heterostructure, *Nano Lett.* **18**, 7651-7657 (2018).

[44] Alberto Ciarrocchi, Dmitrii Unuchek, Ahmet Avsar, Kenji Watanabe, Takashi Taniguchi, Andras Kis, Polarization switching and electrical control of interlayer excitons in two-dimensional van der Waals heterostructures, *Nature Photonics* **13**, 131-136 (2019).

[45] Kyle L. Seyler, Pasqual Rivera, Hongyi Yu, Nathan P. Wilson, Essance L. Ray, David G. Mandrus, Jiaqiang Yan, Wang Yao, Xiaodong Xu, Signatures of moiré-trapped valley excitons in $MoSe_2/WSe_2$ heterobilayers, *Nature* **567**, 66 (2019).

[46] Kha Tran, Galan Moody, Fengcheng Wu, Xiaobo Lu, Junho Choi, Kyounghwan Kim, Amritesh Rai, Daniel A. Sanchez, Jiamin Quan, Akshay Singh, Jacob Embley, André Zepeda, Marshall Campbell, Travis Autry, Takashi Taniguchi, Kenji Watanabe, Nanshu Lu, Sanjay K. Banerjee, Kevin L. Silverman, Suenne Kim, Emanuel Tutuc, Li Yang, Allan H. MacDonald, Xiaoqin Li, Evidence for moiré excitons in van der Waals heterostructures, *Nature* **567**, 71 (2019).

[47] Chenhao Jin, Emma C. Regan, Aiming Yan, M. Iqbal Bakti Utama, Danqing Wang, Sihan Zhao, Ying Qin, Sijie Yang, Zhiren Zheng, Shenyang Shi, Kenji Watanabe, Takashi Taniguchi, Sefaattin Tongay, Alex Zettl, Feng Wang, Observation of moiré excitons in WSe_2/WS_2 heterostructure superlattices, *Nature* **567**, 76 (2019).

[48] Evgeny M. Alexeev, David A. Ruiz-Tijerina, Mark

Danovich, Matthew J. Hamer, Daniel J. Terry, Pramoda K. Nayak, Seongjoon Ahn, Sangyeon Pak, Juwon Lee, Jung Inn Sohn, Maciej R. Molas, Maciej Koperski, Kenji Watanabe, Takashi Taniguchi, Kostya S. Novoselov, Roman V. Gorbachev, Hyeon Suk Shin, Vladimir I. Fal'ko, Alexander I. Tartakovskii, Resonantly hybridized excitons in moiré superlattices in van der Waals heterostructures, *Nature* **567**, 81 (2019).

[49] Chenhao Jin, Emma C. Regan, Danqing Wang, M. Iqbal Bakti Utama, Chan-Shan Yang, Jeffrey Cain, Ying Qin, Yuxia Shen, Zhiren Zheng, Kenji Watanabe, Takashi Taniguchi, Sefaattin Tongay, Alex Zettl, Feng Wang, Resolving spin, valley, and moiré quasi-angular momentum of interlayer excitons in WSe_2/WS_2 heterostructures, arxiv:1902.05887

[50] Fengcheng Wu, Timothy Lovorn, A.H. MacDonald, Topological Exciton Bands in Moiré Heterojunctions, *Phys. Rev. Lett.* **118**, 147401 (2017).

[51] Hongyi Yu, Gui-Bin Liu, Jianju Tang, Xiaodong Xu, Wang Yao, Moiré excitons: From programmable quantum emitter arrays to spin-orbit–coupled artificial lattices, *Sci. Adv.* **3**, e1701696 (2017).

[52] Fengcheng Wu, Timothy Lovorn, A.H. MacDonald, Theory of optical absorption by interlayer excitons in transition metal dichalcogenide heterobilayers, *Phys. Rev. B* **97**, 035306 (2018).

[53] Hongyi Yu, Gui-Bin Liu, Wang Yao, Brightened spin-triplet interlayer excitons and optical selection rules in van der Waals heterobilayers, *2D Mater.* **5**, 035021 (2018).

[54] I.B. Spielman, J.P. Eisenstein, L.N. Pfeiffer, K.W. West, Resonantly Enhanced Tunneling in a Double Layer Quantum Hall Ferromagnet, *Phys. Rev. Lett.* **84**, 5808 (2000).

[55] M. Kellogg, J.P. Eisenstein, L.N. Pfeiffer, K.W. West, Vanishing Hall Resistance at High Magnetic Field in a Double-Layer Two-Dimensional Electron System, *Phys. Rev. Lett.* **93**, 036801 (2004).

[56] E. Tutuc, M. Shayegan, D.A. Huse, Counterflow Measurements in Strongly Correlated GaAs Hole Bilayers: Evidence for Electron-Hole Pairing, *Phys. Rev. Lett.* **93**, 036802 (2004).

[57] J.P. Eisenstein, A.H. MacDonald, Bose-Einstein condensation of excitons in bilayer electron systems, *Nature* **432**, 691-694 (2004).

[58] L. Tiemann, J.G.S. Lok, W. Dietsche, K. von Klitzing, K. Muraki, D. Schuh, W. Wegscheider, Exciton condensate at a total filling factor of one in Corbino two-dimensional electron bilayers, *Phys. Rev. B* **77**, 033306 (2008).

[59] D. Nandi, A.D.K. Finck, J.P. Eisenstein, L.N. Pfeiffer, K.W. West, Exciton condensation and perfect Coulomb drag, *Nature* **488**, 481 (2012).

[60] Xiaomeng Liu, Kenji Watanabe, Takashi Taniguchi, Bertrand I. Halperin, Philip Kim, Quantum Hall drag of exciton condensate in graphene, *Nature Phys.* **13**, 746 (2017).

[61] J.I.A. Li, T. Taniguchi, K. Watanabe, J. Hone, C.R. Dean, Excitonic superfluid phase in double bilayer graphene, *Nature Phys.* **13**, 751 (2017).

[62] Thorsten Deilmann, Kristian Sommer Thygesen, Interlayer Trions in the MoS_2/WS_2 van der Waals Heterostructure, *Nano Lett.* **18**, 1460 (2018).

[63] Gui-Bin Liu, Wen-Yu Shan, Yugui Yao, Wang Yao, Di Xiao, Three-band tight-binding model for monolayers of group-VIB transition metal dichalcogenides, *Phys. Rev. B* **88**, 085433 (2013).

[64] Gang Wang, Cedric Robert, Aslihan Suslu, Bin Chen, Sijie Yang, Sarah Alamdari, Iann C. Gerber, Thierry Amand, Xavier Marie, Sefaattin Tongay, Bernhard Urbaszek, Spin-orbit engineering in transition metal dichalcogenide alloy monolayers, *Nature Commun.* **6**, 10110 (2015).

[65] Xiao-Xiao Zhang, Yumeng You, Shu Yang Frank Zhao, Tony F. Heinz, Experimental Evidence for Dark Excitons in Monolayer WSe_2, *Phys. Rev. Lett.* **115**, 257403 (2015).

[66] You Zhou, Giovanni Scuri, Dominik S. Wild, Alexander A. High, Alan Dibos, Luis A. Jauregui, Chi Shu, Kristiaan De Greve, Kateryna Pistunova, Andrew Y. Joe, Takashi Taniguchi, Kenji Watanabe, Philip Kim, Mikhail D. Lukin, Hongkun Park, Probing dark excitons in atomically thin semiconductors via near-field coupling to surface plasmon polaritons, *Nature Nano.* **12**, 856 (2017).

[67] Xiao-Xiao Zhang, Ting Cao, Zhengguang Lu, Yu-Chuan Lin, Fan Zhang, Ying Wang, Zhiqiang Li, James C. Hone, Joshua A. Robinson, Dmitry Smirnov, Steven G. Louie, Tony F. Heinz, Magnetic brightening and control of dark excitons in monolayer WSe_2, *Nature Nano.* **12**, 883 (2017).

[68] T. Huber, A. Zrenner, W. Wegscheider, M. Bichler, Electrostatic exciton traps, *Phys. Status Solidi A* **166**, R5-R6 (1998).

[69] A.V. Gorbunov, V.B. Timofeev, Interwell excitons in a lateral potential well in an inhomogeneous electric field, *JETP Lett.* **80**, 185-189 (2004).

[70] A.A. High, A.T. Hammack, L.V. Butov, L. Mouchliadis, A.L. Ivanov, M. Hanson, A.C. Gossard, Indirect excitons in elevated traps, *Nano Lett.* **9**, 2094-2098 (2009).

[71] A.A. High, J.R. Leonard, M. Remeika, L.V. Butov, M. Hanson, A.C. Gossard, Condensation of Excitons in a Trap, *Nano Lett.* **12**, 2605 (2012).

[72] G.J. Schinner, J. Repp, E. Schubert, A.K. Rai, D. Reuter, A.D. Wieck, A.O. Govorov, A.W. Holleitner, J.P. Kotthaus, Confinement and interaction of single indirect excitons in a voltage-controlled trap formed inside double InGaAs quantum wells, *Phys. Rev. Lett.* **110**, 127403 (2013).

[73] Y. Shilo, K. Cohen, B. Laikhtman, K. West, L. Pfeiffer, R. Rapaport, Particle correlations and evidence for dark state condensation in a cold dipolar exciton fluid, *Nature Commun.* **4**, 2335 (2013).

[74] Y. Mazuz-Harpaz, K. Cohen, B. Laikhtman, R. Rapaport, K. West, L.N. Pfeiffer, Radiative lifetimes of dipolar excitons in double quantum wells, *Phys. Rev. B* **95**, 155302 (2017).

[75] Z.Y. Zhu, Y.C. Cheng, U. Schwingenschlögl, Giant spin-orbit-induced spin splitting in two-dimensional transition-metal dichalcogenide semiconductors, *Phys. Rev. B* **84**, 153402 (2011).

[76] O. Witham, R.J. Hunt, N.D. Drummond, Stability of trions in coupled quantum wells modeled by two-dimensional bilayers, *Phys. Rev. B* **97**, 075424 (2018).

[77] Igor V. Bondarev, Maria R. Vladimirova, Complexes of dipolar excitons in layered quasi-two-dimensional nanostructures, *Phys. Rev. B* **97**, 165419 (2018).

[78] Kin Fai Mak, Keliang He, Changgu Lee, Gwan Hyoung Lee, James Hone, Tony F. Heinz, Jie Shan, Tightly bound trions in monolayer MoS_2, *Nature Mat.* **12**, 207 (2013).

[79] Jason S. Ross, Sanfeng Wu, Hongyi Yu, Nirmal J. Ghimire, Aaron M. Jones, Grant Aivazian, Jiaqiang Yan, David G. Mandrus, Di Xiao, Wang Yao, Xiaodong Xu, Electrical control of neutral and charged excitons in a monolayer semiconductor, *Nature Commun.* **4**, 1474 (2013).

[80] Timothy C. Berkelbach, Mark S. Hybertsen, David R. Reichman, Theory of neutral and charged excitons in mono-

layer transition metal dichalcogenides, *Phys. Rev. B* **88**, 045318 (2013).

[81] E. Courtade, M. Semina, M. Manca, M.M. Glazov, C. Robert, F. Cadiz, G. Wang, T. Taniguchi, K. Watanabe, M. Pierre, W. Escoffier, E.L. Ivchenko, P. Renucci, X. Marie, T. Amand, B. Urbaszek, Charged excitons in monolayer WSe_2: Experiment and theory, *Phys. Rev. B* **96**, 085302 (2017).

[82] D. Yoshioka, A.H. MacDonald, Double quantum well electron-hole systems in strong magnetic fields, *J. Phys. Soc. Jpn.* **59**, 4211 (1990).

[83] X. Zhu, P.B. Littlewood, M.S. Hybertsen, T.M. Rice, Exciton condensate in semiconductor quantum well structures, *Phys. Rev. Lett.* **74**, 1633 (1995).

[84] Yu.E. Lozovik, O.L. Berman, Phase transitions in a system of two coupled quantum wells, *JETP Lett.* **64**, 573 (1996).